

# Modeling, migration, and inversion in the generalized source and receiver domain

*Yaxun Tang*

## ABSTRACT

I extend the theory of Born modeling, migration and inversion to the generalized source and receiver domain, a transformed domain that is obtained by linear combination of the encoded sources and receivers. I show how to construct the target-oriented imaging Hessian with encoded sources, with encoded receivers and with simultaneously encoded sources and receivers. I also demonstrate the connection of the imaging Hessian in the generalized source and receiver domain to the phase-encoded Hessian that I developed in *SEP-134*. As an application of the theory, I introduce a mixed phase-encoding scheme to compute the Hessian operator. The new scheme combines the advantages of both random phase encoding and plane-wave phase encoding. My preliminary tests of this new method on a simple model show promising results.

## INTRODUCTION

Shot-profile migration is an accurate imaging technique. The computation is performed in each shot gather; thus it closely mimics the actual physical experiment. However, migrating shot by shot is expensive, since the number of shot gathers is usually very big for a typical seismic survey. To reduce the cost, Whitmore (1995), Zhang et al. (2005) and Duquet and Lailly (2006) develop plane-wave source or delayed-shot migration, which migrates a small number of synthesized shots made by linear combination of the original shot gathers after linear time delays. In fact, plane-wave source or delayed-shot migration is only a special case of a more general class of migration technique, phase-encoding migration (Romero et al., 2000; Liu et al., 2006), where the source encoding functions can be any type of phase functions, such as linear phase functions, random phase functions, etc.. Though the methods mentioned above involve encoding only the original sources, there is no reason that the receivers could not be encoded. For example, besides assuming tilted line sources (plane-wave source or delayed-shot migration), we can also assume the data are recorded by tilted line receivers, or assume both line sources and line receivers at the same time. Such ideas have been explored by Stoffa et al. (2006), who develop the ray-based asymptotic theory for plane-wave source migration, plane-wave receiver migration and plane-wave source and receiver migration. In this paper, I extend those ideas from the plane-wave domain to more general cases and unify them under the generalized source and receiver domain.

Another important aspect of imaging is how to preserve the amplitude information of the reflectors. It is widely known that because of the non-unitary nature of the Born forward modeling operator, its adjoint, the migration operator, can only preserve the kinematic information of the reflectors (Lailly, 1983). To better preserve the amplitude, the inversion should be used. Bleistein (2007) derives closed-form asymptotic inversion formulas based on the synthesized shot gathers (e.g. plane-wave sources) under the assumption that the acquisition geometry is infinite. However, we never have infinite acquisition geometry in practice. In fact, the limited acquisition geometry is an important factor distorting the amplitude of the reflectors, especially in complex geologies; hence it should not be neglected.

In this paper, I also extend the target-oriented inversion theory (Valenciano, 2008) to the generalized source and receiver domain for limited acquisition geometry. The effect of limited acquisition geometry is then taken into account in the least-squares sense and corrected by the pseudo-inverse of the target-oriented Hessian, the second derivative of the least-squares misfit functional with respect to the model parameters (Plessix and Mulder, 2004; Valenciano, 2008; Tang, 2008). I demonstrate that in the generalized source and receiver domain, the target-oriented Hessian can be more efficiently computed without storing the Green's functions, which is a major obstacle for the Hessian computation in the original shot-profile domain. I also show that the Hessian obtained in the generalized source and receiver domain is essentially the same as the phase-encoded Hessian (Tang, 2008), the physics of which, however, was not carefully discussed in Tang (2008). Therefore, from this perspective, this paper completes the discussion of the phase-encoded Hessian from the physical point of view. The modeling, migration and target-oriented Hessian formulas are all derived in terms of Green's functions, so that any type of Green's functions can be used under this framework, such as ray-based asymptotic Green's functions, Green's functions obtained by solving one-way wave equations, and Green's functions obtained by solving two-way wave equations. Anisotropy can also be taken into account, provided that the Green's functions are properly modeled.

This paper is organized as follows: I first briefly review the theory of Born modeling, migration and the target-oriented Hessian in the original shot-profile domain. Then I extend the theory to the encoded source domain, the encoded receiver domain, and the encoded source and receiver domain. Finally, I introduce a new phase-encoding scheme, which mixes both random and plane-wave phase encoding, to compute the Hessian operator. The new scheme combines advantages of both random phase encoding and plane-wave phase encoding. Finally, I apply the mixed phase-encoding scheme to a simple synthetic model.

## BORN MODELING AND INVERSION IN THE SHOT-PROFILE DOMAIN

By using the Born approximation to the two-way wave equation, the primaries can be modeled by a linear operator as follows:

$$d(\mathbf{x}_r, \mathbf{x}_s, \omega) = \sum_{\mathbf{x}} G(\mathbf{x}, \mathbf{x}_s, \omega) G(\mathbf{x}, \mathbf{x}_r, \omega) m(\mathbf{x}), \quad (1)$$

where  $d(\mathbf{x}_r, \mathbf{x}_s, \omega)$  is the modeled data for a single frequency  $\omega$  with source and receiver located at  $\mathbf{x}_s = (x_s, y_s, 0)$  and  $\mathbf{x}_r = (x_r, y_r, 0)$  on the surface;  $G(\mathbf{x}, \mathbf{x}_s, \omega)$  and  $G(\mathbf{x}, \mathbf{x}_r, \omega)$  are the Green's functions connecting the source and receiver, respectively, to the image point  $\mathbf{x} = (x, y, z)$  in the subsurface; and  $m(\mathbf{x})$  denotes the reflectivity at image point  $\mathbf{x}$ . In Equation 1, we assume  $\mathbf{x}_s$  and  $\mathbf{x}_r$  are infinite in extent and independent of each other. For a particular survey, however, we do not have infinitely long cable and infinitely many sources; thus we have to introduce an acquisition mask matrix to limit the size of the modeling. We define

$$w(\mathbf{x}_r, \mathbf{x}_s) = \begin{cases} 1 & \text{if } \mathbf{x}_r \text{ is within the recording range of a shot at } \mathbf{x}_s; \\ 0 & \text{otherwise.} \end{cases} \quad (2)$$

For the marine acquisition geometry,  $w(\mathbf{x}_r, \mathbf{x}_s)$  is similar to a band-limited diagonal matrix; for Ocean Bottom Cable (OBC) or land acquisition geometry, where all shots share the same receiver array,  $w(\mathbf{x}_r, \mathbf{x}_s)$  is a rectangular matrix. Figure 1 illustrates the acquisition mask matrices for these two typical geometries in 2-D cases.

To find a model that best fits the observed data, we can minimize the following data-misfit function in the least-squares sense:

$$J(m(\mathbf{x})) = \frac{1}{2} \sum_{\omega} \sum_{\mathbf{x}_s} \sum_{\mathbf{x}_r} |w(\mathbf{x}_r, \mathbf{x}_s) (d(\mathbf{x}_r, \mathbf{x}_s, \omega) - d_{\text{obs}}(\mathbf{x}_r, \mathbf{x}_s, \omega))|^2. \quad (3)$$

The gradient of the above objective function gives the conventional shot-profile migration algorithm:

$$\nabla J(\mathbf{x}) = \Re \left( \sum_{\omega} \sum_{\mathbf{x}_s} G'(\mathbf{x}, \mathbf{x}_s, \omega) \sum_{\mathbf{x}_r} G'(\mathbf{x}, \mathbf{x}_r, \omega) w'(\mathbf{x}_r, \mathbf{x}_s) r(\mathbf{x}_r, \mathbf{x}_s, \omega) \right), \quad (4)$$

where  $\Re$  denotes the real part of a complex number and  $'$  means the complex conjugate;  $r(\mathbf{x}_r, \mathbf{x}_s, \omega)$  is the weighted residual defined as follows:

$$r(\mathbf{x}_r, \mathbf{x}_s, \omega) = w(\mathbf{x}_r, \mathbf{x}_s) (d(\mathbf{x}_r, \mathbf{x}_s, \omega) - d_{\text{obs}}(\mathbf{x}_r, \mathbf{x}_s, \omega)). \quad (5)$$

The gradient or migration is only a rough estimate of the model  $m(\mathbf{x})$ ; to get a better recovery of the model space, the inverse of the Hessian, the second derivatives of the objective function, should be applied to the gradient:

$$\mathbf{m} \approx \mathbf{H}^{-1} \nabla J. \quad (6)$$

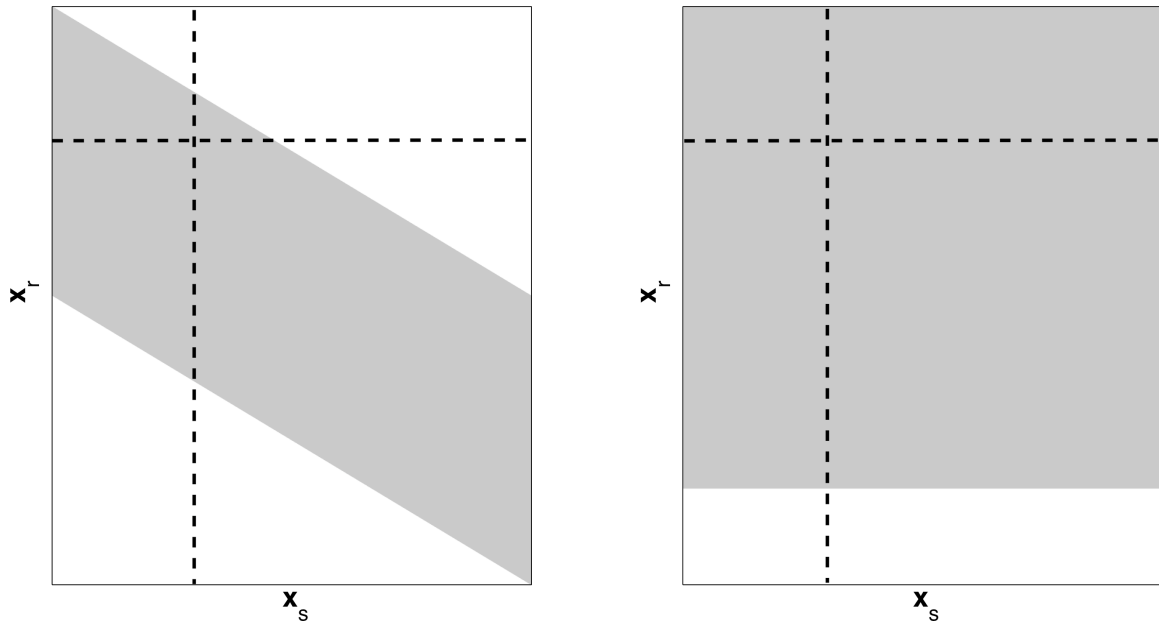


Figure 1: Acquisition mask matrices for different geometries in 2-D cases. Greys denote ones while whites denote zeros. The left panel shows the acquisition mask matrix for a typical marine acquisition geometry; the right panel shows the acquisition mask matrix for a typical OBC or land acquisition geometry. [NR]

The Hessian can be explicitly constructed by taking the second-order derivatives of the objective function with respect to the model parameters as follows (Plessix and Mulder, 2004; Valenciano, 2008; Tang, 2008):

$$H(\mathbf{x}, \mathbf{y}) = \Re \left( \sum_{\omega} \sum_{\mathbf{x}_s} G(\mathbf{x}, \mathbf{x}_s, \omega) G'(\mathbf{y}, \mathbf{x}_s, \omega) \times \sum_{\mathbf{x}_r} w^2(\mathbf{x}_r, \mathbf{x}_s) G(\mathbf{x}, \mathbf{x}_r, \omega) G'(\mathbf{y}, \mathbf{x}_r, \omega) \right), \quad (7)$$

where  $\mathbf{y}$  is a neighbor point around the image point  $\mathbf{x}$  in the subsurface.

Valenciano (2008) demonstrates that the Hessian can be directly computed using the above formula; however it requires storing a large number of Green's functions, which is inconvenient for dealing with large 3-D data set. Tang (2008) shows that with some minor alteration of Equation 7, an approximate Hessian can be efficiently computed using the phase-encoding method. However, Tang (2008) focuses more on the algorithm development, and the physics behind the Hessian by phase-encoding has not been carefully discussed. In this companion paper, I complete the discussion of the actual physics behind using phase-encoding methods, such as plane-wave phase encoding and random phase encoding, to obtain the Hessian. In the subsequent sections, I start with the modeling equation in the encoded source, encoded receiver and simultaneously encoded source and receiver domains. I show that the corresponding

imaging Hessian in the generalized source and receiver domain is the same as those phase-encoded Hessians discussed in Tang (2008).

## ENCODED SOURCES

Let us define the encoding transform along the  $\mathbf{x}_s$  coordinate of the surface data as follows:

$$d(\mathbf{x}_r, \mathbf{p}_s, \omega) = \sum_{\mathbf{x}_s} w(\mathbf{x}_r, \mathbf{x}_s) d(\mathbf{x}_r, \mathbf{x}_s, \omega) \alpha(\mathbf{x}_s, \mathbf{p}_s, \omega), \quad (8)$$

where  $\alpha(\mathbf{x}_s, \mathbf{p}_s, \omega)$  is the source phase-encoding function. Equation 8 integrates along the horizontal dashed lines shown in Figure 1 for each receiver location  $\mathbf{x}_r$  and transforms the surface data from  $(\mathbf{x}_s, \mathbf{x}_r)$  domain into the  $(\mathbf{p}_s, \mathbf{x}_r)$  domain. For the plane-wave phase encoding, the encoding function is:

$$\alpha(\mathbf{x}_s, \mathbf{p}_s, \omega) = e^{i\omega \mathbf{p}_s \mathbf{x}_s}, \quad (9)$$

where  $\mathbf{p}_s$  is defined to be the ray parameter of the source plane waves. For random phase encoding, the encoding function is

$$\alpha(\mathbf{x}_s, \mathbf{p}_s, \omega) = e^{i\gamma(\mathbf{x}_s, \mathbf{p}_s, \omega)}, \quad (10)$$

where  $\gamma(\mathbf{x}_s, \mathbf{p}_s, \omega)$  is a random sequence in  $\mathbf{x}_s$  and  $\omega$ , and  $\mathbf{p}_s$  defines the index of different realizations of the random sequence.

Substituting Equation 1 into 8, rearranging the order of summation, we get the forward modeling equation in the encoded source domain:

$$d(\mathbf{x}_r, \mathbf{p}_s, \omega) = \sum_{\mathbf{x}} G(\mathbf{x}, \mathbf{x}_r, \omega) G(\mathbf{x}, \mathbf{p}_s, \omega; \mathbf{x}_r) m(\mathbf{x}), \quad (11)$$

where the encoded source Green's function  $G(\mathbf{x}, \mathbf{p}_s, \omega; \mathbf{x}_r)$  is defined as follows:

$$G(\mathbf{x}, \mathbf{p}_s, \omega; \mathbf{x}_r) = \sum_{\mathbf{x}_s} w(\mathbf{x}_r, \mathbf{x}_s) G(\mathbf{x}, \mathbf{x}_s, \omega) \alpha(\mathbf{x}_s, \mathbf{p}_s, \omega). \quad (12)$$

Note that  $G(\mathbf{x}, \mathbf{p}_s, \omega; \mathbf{x}_r)$  depends on  $\mathbf{x}_r$  because of the acquisition mask  $w(\mathbf{x}_r, \mathbf{x}_s)$  inside the summation. It should only integrate the grey segment for each horizontal dashed line shown in Figure 1.

As derived in Appendix A, the objective function in the encoded source domain can be written as follows:

$$J(m(\mathbf{x})) = \frac{1}{2} \sum_{\omega} |c|^2 \sum_{\mathbf{x}_r} \sum_{\mathbf{p}_s} |d(\mathbf{x}_r, \mathbf{p}_s, \omega) - d_{\text{obs}}(\mathbf{x}_r, \mathbf{p}_s, \omega)|^2, \quad (13)$$

where  $c = \omega$  for plane-wave phase encoding, and  $c = 1$  for random phase encoding.

The gradient of the objective function in Equation 13 gives the following migration formula in the encoded source domain:

$$\nabla J(\mathbf{x}) = \Re \left( \sum_{\omega} |c|^2 \sum_{\mathbf{p}_s} G'(\mathbf{x}, \mathbf{p}_s, \omega; \mathbf{x}_r) \sum_{\mathbf{x}_r} G'(\mathbf{x}, \mathbf{x}_r, \omega) r(\mathbf{x}_r, \mathbf{p}_s, \omega) \right), \quad (14)$$

where the residual  $r(\mathbf{x}_r, \mathbf{p}_s, \omega)$  is defined as follows:

$$r(\mathbf{x}_r, \mathbf{p}_s, \omega) = d(\mathbf{x}_r, \mathbf{p}_s, \omega) - d_{\text{obs}}(\mathbf{x}_r, \mathbf{p}_s, \omega). \quad (15)$$

It is easy to see that Equation 14 defines the phase-encoding migration (Liu et al., 2006; Romero et al., 2000). By taking the second-order derivatives of the objective function defined in Equation 13 with respect to the model parameters, we obtain the Hessian in the encoded source domain:

$$H(\mathbf{x}, \mathbf{y}) = \Re \left( \sum_{\omega} |c|^2 \sum_{\mathbf{x}_r} G(\mathbf{x}, \mathbf{x}_r, \omega) G'(\mathbf{y}, \mathbf{x}_r, \omega) \times \sum_{\mathbf{p}_s} G(\mathbf{x}, \mathbf{p}_s, \omega; \mathbf{x}_r) G'(\mathbf{y}, \mathbf{p}_s, \omega; \mathbf{x}_r) \right). \quad (16)$$

## ENCODED RECEIVERS

Let us define the encoding transform along the  $\mathbf{x}_r$  coordinate of the surface data as follows:

$$d(\mathbf{p}_r, \mathbf{x}_s, \omega) = \sum_{\mathbf{x}_r} w(\mathbf{x}_r, \mathbf{x}_s) d(\mathbf{x}_r, \mathbf{x}_s, \omega) \beta(\mathbf{x}_r, \mathbf{p}_r, \omega), \quad (17)$$

where  $\beta(\mathbf{x}_r, \mathbf{p}_r, \omega)$  is the receiver phase-encoding function. Equation 17 integrates along the vertical dashed lines shown in Figure 1 for each source location  $\mathbf{x}_s$  and transforms the surface data from  $(\mathbf{x}_s, \mathbf{x}_r)$  domain into the  $(\mathbf{x}_s, \mathbf{p}_r)$  domain. The receiver phase-encoding function is defined similar to the source phase-encoding function discussed in the previous section. For receiver plane-wave phase encoding,

$$\beta(\mathbf{x}_r, \mathbf{p}_r, \omega) = e^{i\omega \mathbf{p}_r \mathbf{x}_r}, \quad (18)$$

where  $\mathbf{p}_r$  is the ray parameter for the receiver plane-waves. For receiver random phase encoding,

$$\beta(\mathbf{x}_r, \mathbf{p}_r, \omega) = e^{i\gamma(\mathbf{x}_r, \mathbf{p}_r, \omega)}, \quad (19)$$

where  $\gamma(\mathbf{x}_r, \mathbf{p}_r, \omega)$  is the  $\mathbf{p}_r$ th random realization. Substituting Equation 1 into 17, we get the forward modeling equation in the receiver plane-wave domain:

$$d(\mathbf{p}_r, \mathbf{x}_s, \omega) = \sum_{\mathbf{x}} G(\mathbf{x}, \mathbf{x}_s, \omega) G(\mathbf{x}, \mathbf{p}_r, \omega; \mathbf{x}_s) m(\mathbf{x}), \quad (20)$$

where  $G(\mathbf{x}, \mathbf{p}_r, \omega; \mathbf{x}_s)$  is the encoded receiver Green's function defined as follows:

$$G(\mathbf{x}, \mathbf{p}_r, \omega; \mathbf{x}_s) = \sum_{\mathbf{x}_r} w(\mathbf{x}_r, \mathbf{x}_s) G(\mathbf{x}, \mathbf{x}_r, \omega) \beta(\mathbf{x}_r, \mathbf{p}_r, \omega). \quad (21)$$

Also note that  $G(\mathbf{x}, \mathbf{p}_r, \omega; \mathbf{x}_s)$  depends on  $\mathbf{x}_s$  because of the acquisition mask matrix inside the summation. It should only integrate the grey segment for each vertical dashed line shown in Figure 1.

We minimize the following objective function in the encoded receiver domain (see Appendix B for derivation):

$$J(m(\mathbf{x})) = \sum_{\omega} |c|^2 \sum_{\mathbf{p}_r} \sum_{\mathbf{x}_s} |d(\mathbf{p}_r, \mathbf{x}_s, \omega) - d_{\text{obs}}(\mathbf{p}_r, \mathbf{x}_s, \omega)|^2, \quad (22)$$

The gradient of the objective function in Equation 22 gives the following migration formula in the encoded receiver domain:

$$\nabla J(\mathbf{x}) = \Re \left( \sum_{\omega} |c|^2 \sum_{\mathbf{x}_s} G'(\mathbf{x}, \mathbf{x}_s, \omega) \sum_{\mathbf{p}_r} G'(\mathbf{x}, \mathbf{p}_r, \omega; \mathbf{x}_s) r(\mathbf{p}_r, \mathbf{x}_s, \omega) \right), \quad (23)$$

where the residual  $r(\mathbf{p}_r, \mathbf{x}_s, \omega)$  is defined as follows:

$$r(\mathbf{p}_r, \mathbf{x}_s, \omega) = d(\mathbf{p}_r, \mathbf{x}_s, \omega) - d_{\text{obs}}(\mathbf{p}_r, \mathbf{x}_s, \omega). \quad (24)$$

The Hessian in the encoded receiver domain is then obtained by taking the second derivative of the objective function:

$$H(\mathbf{x}, \mathbf{y}) = \Re \left( \sum_{\omega} |c|^2 \sum_{\mathbf{x}_s} G(\mathbf{x}, \mathbf{x}_s, \omega) G'(\mathbf{y}, \mathbf{x}_s, \omega) \times \sum_{\mathbf{p}_r} G(\mathbf{x}, \mathbf{p}_r, \omega; \mathbf{x}_s) G'(\mathbf{y}, \mathbf{p}_r, \omega; \mathbf{x}_s) \right). \quad (25)$$

We can rewrite Equation 25 as follows

$$H(\mathbf{x}, \mathbf{y}) = \sum_{\mathbf{p}_r} H(\mathbf{x}, \mathbf{y}, \mathbf{p}_r), \quad (26)$$

where

$$\begin{aligned}
H(\mathbf{x}, \mathbf{y}, \mathbf{p}_r) &= \Re \left( \sum_{\omega} |c|^2 \sum_{\mathbf{x}_s} G(\mathbf{x}, \mathbf{x}_s, \omega) G'(\mathbf{y}, \mathbf{x}_s, \omega) \times \right. \\
&\quad \left. G(\mathbf{x}, \mathbf{p}_r, \omega; \mathbf{x}_s) G'(\mathbf{y}, \mathbf{p}_r, \omega; \mathbf{x}_s) \right) \\
&= \Re \left( \sum_{\omega} |c|^2 \sum_{\mathbf{x}_s} G(\mathbf{x}, \mathbf{x}_s, \omega) G'(\mathbf{y}, \mathbf{x}_s, \omega) \times \right. \\
&\quad \left( \sum_{\mathbf{x}_r} w(\mathbf{x}_r, \mathbf{x}_s) G(\mathbf{x}, \mathbf{x}_r, \omega) \beta(\mathbf{x}_r, \mathbf{p}_r, \omega) \right) \times \\
&\quad \left. \left( \sum_{\mathbf{x}'_r} w(\mathbf{x}_r, \mathbf{x}_s) G(\mathbf{y}, \mathbf{x}'_r, \omega) \beta(\mathbf{x}'_r, \mathbf{p}_r, \omega) \right) \right). \quad (27)
\end{aligned}$$

Equation 27 is equivalent to Equations 9 and B-1 in Tang (2008), which are called the receiver-side encoded Hessian. As I show here, the receiver-side encoded Hessian is the same as the Hessian in the encoded receiver domain; both of them are derived from the same forward modeling equation defined in Equation 20.

## ENCODED SOURCES AND RECEIVERS

We can simultaneously encode the sources and the receivers as follows:

$$d(\mathbf{p}_r, \mathbf{p}_s, \omega) = \sum_{\mathbf{x}_r} \sum_{\mathbf{x}_s} w(\mathbf{x}_r, \mathbf{x}_s) d(\mathbf{x}_r, \mathbf{x}_s, \omega) \alpha(\mathbf{x}_s, \mathbf{p}_s, \omega) \beta(\mathbf{x}_r, \mathbf{p}_r, \omega), \quad (28)$$

where  $\alpha(\mathbf{x}_s, \mathbf{p}_s, \omega)$  and  $\beta(\mathbf{x}_r, \mathbf{p}_r, \omega)$  are defined by Equations 9 and 18, respectively, for plane-wave phase encoding, and by Equations 10 and 19, respectively, for random phase encoding.

Substituting Equations 1 into 28, notice that  $w^2(\mathbf{x}_r, \mathbf{x}_s) = w(\mathbf{x}_r, \mathbf{x}_s)$ . With the definition of  $G(\mathbf{x}, \mathbf{p}_s, \omega; \mathbf{x}_r)$  and  $G(\mathbf{x}, \mathbf{p}_r, \omega; \mathbf{x}_s)$  by Equations 12 and 21, we obtain the forward modeling equation in the encoded source and receiver domain:

$$d(\mathbf{p}_r, \mathbf{p}_s, \omega) = \sum_{\mathbf{x}} G(\mathbf{x}, \mathbf{p}_r, \omega; \mathbf{x}_s) G(\mathbf{x}, \mathbf{p}_s, \omega; \mathbf{x}_r) m(\mathbf{x}). \quad (29)$$

Now we minimize the following objective function in the encoded source and receiver domain (see Appendix C for derivation):

$$J(m(\mathbf{x})) = \sum_{\omega} |c|^4 \sum_{\mathbf{p}_r} \sum_{\mathbf{p}_s} |d(\mathbf{p}_r, \mathbf{p}_s, \omega) - d_{\text{obs}}(\mathbf{p}_r, \mathbf{p}_s, \omega)|^2. \quad (30)$$



The gradient of the objective function in Equation 30 gives the following migration formula in the encoded source and receiver domain:

$$\nabla J(\mathbf{x}) = \Re \left( \sum_{\omega} |c|^4 \sum_{\mathbf{p}_r} G'(\mathbf{x}, \mathbf{p}_r, \omega; \mathbf{x}_s) \sum_{\mathbf{p}_s} G'(\mathbf{x}, \mathbf{p}_s, \omega; \mathbf{x}_r) r(\mathbf{p}_r, \mathbf{p}_s, \omega) \right), \quad (31)$$

where  $r(\mathbf{p}_r, \mathbf{p}_s, \omega)$  is the residual in the encoded source and receiver domain:

$$r(\mathbf{p}_r, \mathbf{p}_s, \omega) = d(\mathbf{p}_r, \mathbf{p}_s, \omega) - d_{\text{obs}}(\mathbf{p}_r, \mathbf{p}_s, \omega). \quad (32)$$

The Hessian is obtained as follows:

$$\begin{aligned} H(\mathbf{x}, \mathbf{y}) = & \Re \left( \sum_{\omega} |c|^4 \sum_{\mathbf{p}_r} G(\mathbf{x}, \mathbf{p}_r, \omega; \mathbf{x}_s) G'(\mathbf{y}, \mathbf{p}_r, \omega; \mathbf{x}_s) \times \right. \\ & \left. \sum_{\mathbf{p}_s} G(\mathbf{x}, \mathbf{p}_s, \omega; \mathbf{x}_r) G'(\mathbf{y}, \mathbf{p}_s, \omega; \mathbf{x}_r) \right). \end{aligned} \quad (33)$$

We can also rewrite Equation 33 as follows:

$$H(\mathbf{x}, \mathbf{y}) = \sum_{\mathbf{p}_s} \sum_{\mathbf{p}_r} H(\mathbf{x}, \mathbf{y}, \mathbf{p}_s, \mathbf{p}_r), \quad (34)$$

where

$$\begin{aligned} & H(\mathbf{x}, \mathbf{y}, \mathbf{p}_s, \mathbf{p}_r) \\ &= \Re \left( \sum_{\omega} |c|^4 G(\mathbf{x}, \mathbf{p}_s, \omega; \mathbf{x}_r) G'(\mathbf{y}, \mathbf{p}_s, \omega; \mathbf{x}_r) G(\mathbf{x}, \mathbf{p}_r, \omega; \mathbf{x}_s) G'(\mathbf{y}, \mathbf{p}_r, \omega; \mathbf{x}_s) \right) \\ &= \Re \left( \sum_{\omega} |c|^4 \times \right. \\ & \quad \left( \sum_{\mathbf{x}_s} w(\mathbf{x}_r, \mathbf{x}_s) G(\mathbf{x}, \mathbf{x}_s, \omega) \alpha(\mathbf{x}_s, \mathbf{p}_s, \omega) \right) \left( \sum_{\mathbf{x}'_s} w(\mathbf{x}_r, \mathbf{x}'_s) G(\mathbf{y}, \mathbf{x}'_s, \omega) \alpha(\mathbf{x}'_s, \mathbf{p}_s, \omega) \right)' \times \\ & \quad \left( \sum_{\mathbf{x}_r} w(\mathbf{x}_r, \mathbf{x}_s) G(\mathbf{x}, \mathbf{x}_r, \omega) \beta(\mathbf{x}_r, \mathbf{p}_r, \omega) \right) \left( \sum_{\mathbf{x}'_r} w(\mathbf{x}'_r, \mathbf{x}_s) G(\mathbf{y}, \mathbf{x}'_r, \omega) \beta(\mathbf{x}'_r, \mathbf{p}_r, \omega) \right)' \right). \end{aligned} \quad (35)$$

Equation 35 is equivalent to Equations 17 and C-1 in Tang (2008), which are called the simultaneously encoded Hessian. However, Equation 35 is more general, because it is not limited to OBC or land acquisition geometry. Up to this point, we have proved that both the simultaneously encoded Hessian and the Hessian in the encoded source and receiver domain are derived from the same forward modeling equation defined in 29.

## A MIXED PHASE-ENCODING SCHEME

Tang (2008) compares the computational cost for the Hessian obtained using different phase-encoding and shows that the most efficient way to compute the Hessian is to use simultaneous random phase encoding. The cost is just two downward continuations (using one-way wave equation to model the Green’s functions) of the encoded wavefields plus the cross-correlation (for a single realization of the random phases). However, the random phase encoding may not be very effective in attenuating the cross-talk when many Green’s functions are simultaneously encoded (Romero et al., 2000; Tang, 2008); a lot of random noise may appear in the final result. In fact, for the simultaneous phase encoding or the Hessian in the encoded source and receiver domain defined by Equation 33, the phase-encoding functions for sources ( $\alpha(\mathbf{x}_s, \mathbf{p}_s, \omega)$ ) and receivers ( $\beta(\mathbf{x}_r, \mathbf{p}_r, \omega)$ ) need not be the same. For example, we can use plane-wave phase encoding function to encode the sources but use random phase-encoding function to encode the receivers, or vice visa. Because plane-wave phase encoding functions are very effective in attenuating the cross-talk (Liu et al., 2006; Tang, 2008), while random phase encoding is efficient, by combining those two phase-encoding functions, we are able to balance cost and accuracy.

I apply this idea to a simple constant-velocity model. The acquisition geometry is assumed to be OBC geometry, where all shots share the same receiver array. There are 201 shots from  $-2000$  m to  $2000$  m with a  $10$  m sampling; for each shot, there are 201 receivers spanning from  $-2000$  m to  $2000$  m. Figure 2 shows the diagonal of the Hessian obtained using different methods. Figure 2(a) shows the exact diagonal of the Hessian computed in the original shot-profile domain with Equation 7, which requires pre-computing and saving the Green’s functions and is efficient for practical applications. However, since there is no cross-talk in the original shot-profile domain, I use the result as a benchmark to compare the accuracy of other methods. Figure 2(b) is obtained using the most efficient simultaneous random phase-encoding method (only one realization of the random-phase functions has been used), by using Equation 33, with both  $\alpha(\mathbf{x}_s, \mathbf{p}_s, \omega)$  and  $\beta(\mathbf{x}_r, \mathbf{p}_r, \omega)$  being random phase functions. As expected, the result is full of random noise, useful illumination information is greatly distorted, and the result is very far from the exact Hessian. Figure 2(c) shows the result obtained using the mixed phase-encoding scheme, i.e., by using Equation 33, with the weighting function  $\alpha(\mathbf{x}_s, \mathbf{p}_s, \omega)$  being the plane-wave phase-encoding function and  $\beta(\mathbf{x}_r, \mathbf{p}_r, \omega)$  being the random phase-encoding function. A total of 61 plane-wave-encoded source-side Green’s functions have been used to generate the result. The cost is the same as a plane-wave source migration with 61 source plane waves. The result looks very similar to the exact Hessian, and the random noise shown in Figure 2(b) has been greatly reduced. For comparison, Figure 2(d) shows the Hessian computed in the encoded receiver domain, i.e., by using Equation 25, where the weighting function  $\beta(\mathbf{x}_r, \mathbf{p}_r, \omega)$  is chosen to be a random phase function. The result is also very accurate. However, its cost is the same as a shot-profile migration with 201 shot gathers (Tang, 2008).

Figure 3 and 4 show the Hessian with off-diagonals (with size  $21 \times 21$ ) obtained us-

ing different methods. Figure 3 illustrates the result at image point ( $x = 0, z = 800$ ), while Figure 4 illustrates the result at image point ( $x = 420, z = 800$ ). These results also demonstrate that although simultaneous random phase encoding is efficient, the Hessian operator obtained by this method (Figure 3(b) and Figure 4(b)) suffers a lot from unwanted crosstalk. Encoding only the receiver-side Green's function with random phase functions gives accurate results (Figure 3(d) and Figure 4(d)); however, the cost is similar to a shot-profile migration. In situations where the number of shot gathers is big, this encoding scheme may not be a good choice. In contrast, the mixed phase-encoding scheme gives us very accurate results (Figure 3(c) and Figure 4(c)) but with less cost than the receiver-side encoded Hessian.

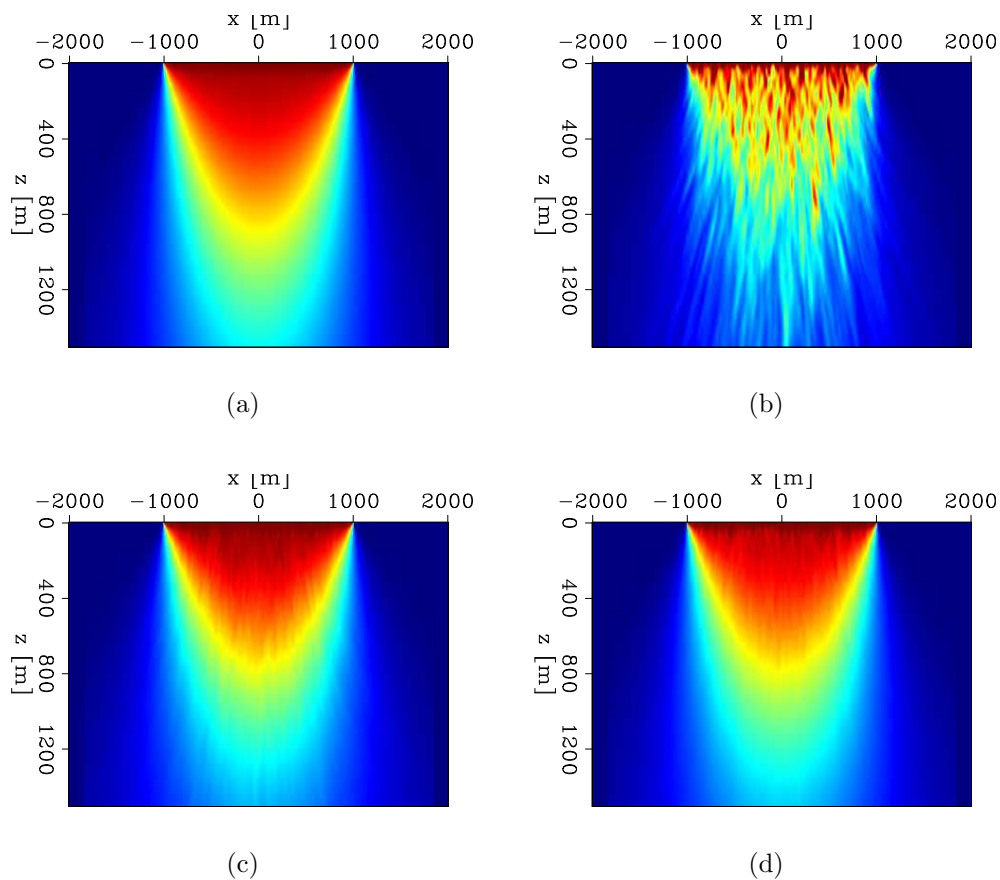


Figure 2: The diagonal of the Hessian obtained with different methods. Panel (a) is the exact diagonal of Hessian computed in the original shot-profile domain. Panel (b) is the result computed in the encoded source and receiver domain, where both the source and receiver Green's functions are randomly encoded. Panel (c) is the result also computed in the encoded source and receiver domain, where the source-side Green's functions are encoded with the plane-wave phase encoding function, while the receiver-side Green's functions are encoded with the random phase functions. Panel (d) is the result computed in the encoded receiver domain, where only the receiver-side Green's functions are randomly encoded. **[CR]**

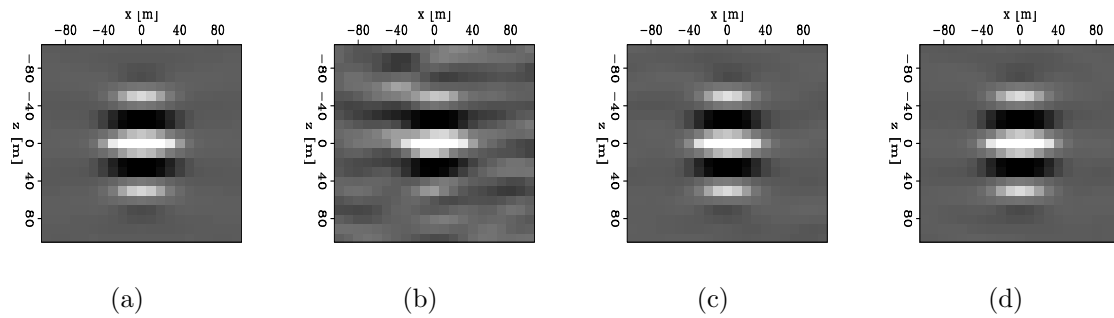


Figure 3: The Hessian operator for an image point at  $x = 0$  m and  $z = 800$  m, with the same acquisition geometry as in Figure 2. The size of the Hessian operator is  $21 \times 21$ . Panel (a) shows the exact Hessian computed in the original shot-profile domain, which is artifact-free; Panel (b) is the result of simultaneous random phase encoding. Note the strong artifact which distorts the useful information; Panel (c) is the result of the mixed phase encoding; the result is very similar to the exact Hessian in (a); Panel (d) is the result computed in the encoded receiver domain, where only the receiver-side Green's functions are randomly encoded. [CR]

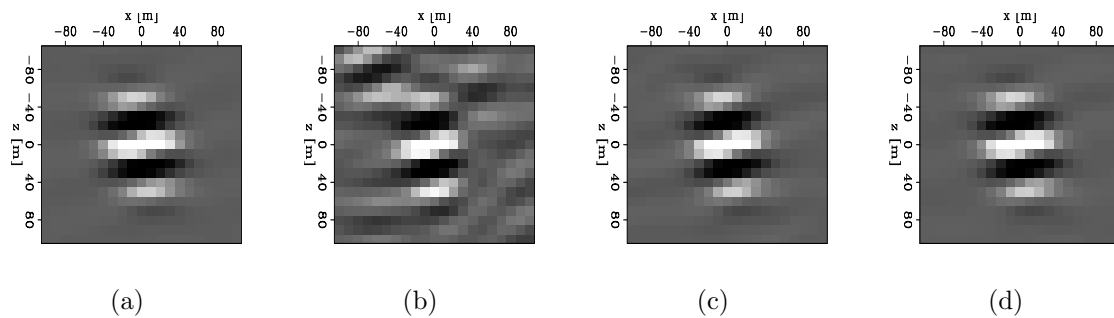


Figure 4: The Hessian operator for an image point at  $x = 420$  m and  $z = 800$  m, with the same acquisition geometry as in Figure 2. The size of the Hessian operator is  $21 \times 21$ . Panel (a) shows the exact Hessian computed in the original shot-profile domain, which is artifact-free; Panel (b) is the result of simultaneous random phase encoding. Note the strong artifact which distorts the useful information; Panel (c) is the result of the mixed phase encoding; the result is very similar to the exact Hessian in (a); Panel (d) is the result computed in the encoded receiver domain, where only the receiver-side Green's functions are randomly encoded. [CR]

## CONCLUSION

I extend the theory of Born modeling, migration and inversion from the conventional shot-profile domain to the generalized source and receiver domain, and to the plane-wave phase-encoding domain and the random phase-encoding domain in particular. One important advantage of these new domains is that computing the target-oriented Hessian no longer requires storing the Green's functions, which is a major obstacle preventing the Hessian computation in the original shot-profile domain. I also prove that the Hessians obtained in the generalized source and receiver domain are equivalent to those phase-encoded Hessians discussed in Tang (2008), and they both can be derived from the same modeling equations. To balance the accuracy and cost of computing the Hessian, I introduce a new phase encoding domain, i.e., the mixed phase-encoding scheme, which combines plane-wave phase encoding and random phase encoding. My preliminary tests shows that this new phase-encoding scheme achieves high accuracy with relatively low cost.

## REFERENCES

- Bleistein, N., 2007, Migration/inversion for incident waves synthesized from common-shot data gathers: *Geophysics*, **72**, W17–W31.
- Duquet, B. and P. Lailly, 2006, Efficient 3D wave-equation migration using virtual planar sources: *Geophysics*, **71**, S185–S197.
- Lailly, P., 1983, The seismic inverse problem as a sequence of before stack migration: Proc. Conf. on Inverse Scattering, Theory and Applications, Expanded Abstracts, Philadelphia, SIAM.
- Liu, F., D. W. Hanson, N. D. Whitmore, R. S. Day, and R. H. Stolt, 2006, Toward a unified analysis for source plane-wave migration: *Geophysics*, **71**, S129–S139.
- Plessix, R.-E. and W. A. Mulder, 2004, Frequency-domain finite-difference amplitude-preserving migration: *Geophys. J. Int.*, **157**, 975–987.
- Romero, L. A., D. C. Ghiglia, C. C. Ober, and S. A. Morton, 2000, Phase encoding of shot records in prestack migration: *Geophysics*, **65**, 426–436.
- Stoffa, P. L., M. K. Sen, R. K. Seifoullaev, R. C. Pestana, and J. T. Fokkema, 2006, Plane-wave depth migration: *Geophysics*, **71**, S261–S272.
- Tang, Y., 2008, Wave-equation Hessian by phase encoding: **SEP-134**, 1–24.
- Valenciano, A., 2008, Imaging by Wave-equation Inversion: PhD thesis, Stanford University.
- Whitmore, N. D., 1995, An Imaging Hierarchy for Common Angle Plane Wave Seismogram: PhD thesis, University of Tulsa.
- Zhang, Y., J. Sun, C. Notfors, S. Grey, L. Chemis, and J. Young, 2005, Delayed-shot 3D depth migration: *Geophysics*, **70**, E21–E28.

## APPENDIX A

This appendix derives the objective function in the encoded source domain. We start with the objective function in the source and receiver domain as follows:

$$J(m(\mathbf{x})) = \frac{1}{2} \sum_{\omega} \sum_{\mathbf{x}_s} \sum_{\mathbf{x}_r} |w(\mathbf{x}_r, \mathbf{x}_s)(d(\mathbf{x}_r, \mathbf{x}_s, \omega) - d_{\text{obs}}(\mathbf{x}_r, \mathbf{x}_s, \omega))|^2. \quad (\text{A-1})$$

From Equation 8, we can also get the inverse phase-encoding transform. For source plane-wave phase encoding, since the forward operator is unitary, the inverse transform can be written as follows:

$$w(\mathbf{x}_r, \mathbf{x}_s)d(\mathbf{x}_r, \mathbf{x}_s, \omega) = |\omega|^2 \sum_{\mathbf{p}_s} d(\mathbf{x}_r, \mathbf{p}_s, \omega)e^{-i\omega\mathbf{p}_s\mathbf{x}_s}. \quad (\text{A-2})$$

For random phase encoding, a similar result can also be obtained, because different realizations of random sequences should be approximately orthogonal, provided that those random sequences are "sufficiently" random; thus we have

$$w(\mathbf{x}_r, \mathbf{x}_s)d(\mathbf{x}_r, \mathbf{x}_s, \omega) = \sum_{\mathbf{p}_s} d(\mathbf{x}_r, \mathbf{p}_s, \omega)e^{-i\gamma(\mathbf{x}_s, \mathbf{p}_s, \omega)}. \quad (\text{A-3})$$

Therefore, we can use a more general form to express the inverse phase-encoding transform:

$$w(\mathbf{x}_r, \mathbf{x}_s)d(\mathbf{x}_r, \mathbf{x}_s, \omega) = |c|^2 \sum_{\mathbf{p}_s} d(\mathbf{x}_r, \mathbf{p}_s, \omega)\alpha'(\mathbf{x}_s, \mathbf{p}_s, \omega), \quad (\text{A-4})$$

where for plane-wave phase encoding,  $c = \omega$  and  $\alpha(\mathbf{x}_s, \mathbf{p}_s, \omega) = e^{i\omega\mathbf{p}_s\mathbf{x}_s}$ ; for random phase encoding,  $c = 1$  and  $\alpha(\mathbf{x}_s, \mathbf{p}_s, \omega) = e^{i\gamma(\mathbf{x}_s, \mathbf{p}_s, \omega)}$ .

Substituting Equation A-4 into A-1 yields:

$$\begin{aligned} J(m(\mathbf{x})) &= \frac{1}{2} \sum_{\omega} \sum_{\mathbf{x}_s} \sum_{\mathbf{x}_r} |c|^4 \left| \sum_{\mathbf{p}_s} r(\mathbf{x}_r, \mathbf{p}_s, \omega)\alpha'(\mathbf{x}_s, \mathbf{p}_s, \omega) \right|^2 \\ &= \frac{1}{2} \sum_{\omega} \sum_{\mathbf{x}_s} \sum_{\mathbf{x}_r} |c|^4 \left( \sum_{\mathbf{p}_s} r(\mathbf{x}_r, \mathbf{p}_s, \omega)\alpha'(\mathbf{x}_s, \mathbf{p}_s, \omega) \right)' \times \\ &\quad \left( \sum_{\mathbf{p}'_s} r(\mathbf{x}_r, \mathbf{p}'_s, \omega)\alpha'(\mathbf{x}_s, \mathbf{p}'_s, \omega) \right) \\ &= \frac{1}{2} \sum_{\omega} \sum_{\mathbf{x}_r} |c|^4 \sum_{\mathbf{p}_s} \sum_{\mathbf{p}'_s} r'(\mathbf{x}_r, \mathbf{p}_s, \omega)r(\mathbf{x}_r, \mathbf{p}'_s, \omega) \times \\ &\quad \sum_{\mathbf{x}_s} \alpha(\mathbf{x}_s, \mathbf{p}_s, \omega)\alpha'(\mathbf{x}_s, \mathbf{p}'_s, \omega), \end{aligned} \quad (\text{A-5})$$

where  $r(\mathbf{x}_r, \mathbf{p}_s, \omega)$  is defined to be the residual in the encoded source domain:

$$r(\mathbf{x}_r, \mathbf{p}_s, \omega) = d(\mathbf{x}_r, \mathbf{p}_s, \omega) - d_{\text{obs}}(\mathbf{x}_r, \mathbf{p}_s, \omega). \quad (\text{A-6})$$

For plane-wave phase encoding, if the  $\mathbf{x}_s$  is sampled densely enough,

$$\sum_{\mathbf{x}_s} \alpha(\mathbf{x}_s, \mathbf{p}_s, \omega) \alpha'(\mathbf{x}_s, \mathbf{p}'_s, \omega) = \sum_{\mathbf{x}_s} e^{i\omega(\mathbf{p}'_s - \mathbf{p}_s)\mathbf{x}_s} \approx \frac{1}{|\omega|^2} \delta(\mathbf{p}'_s - \mathbf{p}_s). \quad (\text{A-7})$$

For random phase encoding, the following property also holds as long as the random sequences are "sufficiently" random:

$$\sum_{\mathbf{x}_s} \alpha(\mathbf{x}_s, \mathbf{p}_s, \omega) \alpha'(\mathbf{x}_s, \mathbf{p}'_s, \omega) = \sum_{\mathbf{x}_s} e^{i(\gamma(\mathbf{x}_s, \mathbf{p}'_s, \omega) - \gamma(\mathbf{x}_s, \mathbf{p}_s, \omega))} \approx \delta(\mathbf{p}'_s - \mathbf{p}_s). \quad (\text{A-8})$$

Substituting Equation A-7 or A-8 into A-5, we get the data-misfit function in the encoded source domain:

$$J(m(\mathbf{x})) \approx \frac{1}{2} \sum_{\omega} |c|^2 \sum_{\mathbf{x}_r} \sum_{\mathbf{p}_s} |d(\mathbf{x}_r, \mathbf{p}_s, \omega) - d_{\text{obs}}(\mathbf{x}_r, \mathbf{p}_s, \omega)|^2. \quad (\text{A-9})$$

## APPENDIX B

This appendix derives the objective function in the encoded receiver domain. We start with the objective function in the source and receiver domain as follows:

$$J(m(\mathbf{x})) = \frac{1}{2} \sum_{\omega} \sum_{\mathbf{x}_s} \sum_{\mathbf{x}_r} |w(\mathbf{x}_r, \mathbf{x}_s)(d(\mathbf{x}_r, \mathbf{x}_s, \omega) - d_{\text{obs}}(\mathbf{x}_r, \mathbf{x}_s, \omega))|^2. \quad (\text{B-1})$$

Similar to the discussion in Appendix A, the general form of the inverse transform of receiver phase encoding can be written as follows:

$$w(\mathbf{x}_r, \mathbf{x}_s) d(\mathbf{x}_r, \mathbf{x}_s, \omega) = |c|^2 \sum_{\mathbf{p}_r} d(\mathbf{p}_r, \mathbf{x}_s, \omega) \beta'(\mathbf{x}_r, \mathbf{p}_r, \omega), \quad (\text{B-2})$$

where for plane-wave phase encoding,  $c = \omega$  and  $\beta(\mathbf{x}_r, \mathbf{p}_r, \omega) = e^{i\omega \mathbf{p}_r \mathbf{x}_r}$ ; for random phase encoding,  $c = 1$  and  $\beta(\mathbf{x}_r, \mathbf{p}_r, \omega) = e^{i\gamma(\mathbf{x}_r, \mathbf{p}_r, \omega)}$ . Substituting Equation B-2 into

B-1 yields:

$$\begin{aligned}
J(m(\mathbf{x})) &= \frac{1}{2} \sum_{\omega} \sum_{\mathbf{x}_s} \sum_{\mathbf{x}_r} |c|^4 \left| \sum_{\mathbf{p}_r} r(\mathbf{p}_r, \mathbf{x}_s, \omega) \beta'(\mathbf{x}_r, \mathbf{p}_r, \omega) \right|^2 \\
&= \frac{1}{2} \sum_{\omega} \sum_{\mathbf{x}_s} \sum_{\mathbf{x}_r} |c|^4 \left( \sum_{\mathbf{p}_r} r(\mathbf{p}_r, \mathbf{x}_s, \omega) \beta'(\mathbf{x}_r, \mathbf{p}_r, \omega) \right)' \times \\
&\quad \left( \sum_{\mathbf{p}'_r} r(\mathbf{p}'_r, \mathbf{x}_s, \omega) \beta'(\mathbf{x}_r, \mathbf{p}'_r, \omega) \right) \\
&= \frac{1}{2} \sum_{\omega} \sum_{\mathbf{x}_s} |c|^4 \sum_{\mathbf{p}_r} \sum_{\mathbf{p}'_r} r'(\mathbf{p}_r, \mathbf{x}_s, \omega) r(\mathbf{p}'_r, \mathbf{x}_s, \omega) \times \\
&\quad \sum_{\mathbf{x}_r} \beta(\mathbf{x}_r, \mathbf{p}_r, \omega) \beta'(\mathbf{x}_r, \mathbf{p}'_r, \omega), \tag{B-3}
\end{aligned}$$

where  $r(\mathbf{p}_r, \mathbf{x}_s, \omega)$  is defined to be the residual in the encoded receiver domain:

$$r(\mathbf{p}_r, \mathbf{x}_s, \omega) = d(\mathbf{p}_r, \mathbf{x}_s, \omega) - d_{\text{obs}}(\mathbf{p}_r, \mathbf{x}_s, \omega). \tag{B-4}$$

Similar to the discussion in Appendix A, the inner-most summation in Equation B-3 is approximately a Dirac delta function under certain conditions. Therefore, the data-misfit function in the encoded receiver domain reads as follows:

$$J(m(\mathbf{x})) \approx \frac{1}{2} \sum_{\omega} |c|^2 \sum_{\mathbf{p}_r} \sum_{\mathbf{x}_s} |d(\mathbf{p}_r, \mathbf{x}_s, \omega) - d_{\text{obs}}(\mathbf{p}_r, \mathbf{x}_s, \omega)|^2. \tag{B-5}$$

## APPENDIX C

This appendix derives the objective function in the simultaneously encoded source and receiver domain. We start with the objective function in the source and receiver domain as follows:

$$J(m(\mathbf{x})) = \frac{1}{2} \sum_{\omega} \sum_{\mathbf{x}_s} \sum_{\mathbf{x}_r} |w(\mathbf{x}_r, \mathbf{x}_s) (d(\mathbf{x}_r, \mathbf{x}_s, \omega) - d_{\text{obs}}(\mathbf{x}_r, \mathbf{x}_s, \omega))|^2. \tag{C-1}$$

If we follow a discussion similar to those in Appendices A and B, we obtain the general expression of the inverse transform of the simultaneous encoding:

$$w(\mathbf{x}_r, \mathbf{x}_s, \omega) d(\mathbf{x}_r, \mathbf{x}_s, \omega) = |c|^4 \sum_{\mathbf{p}_s} \sum_{\mathbf{p}_r} d(\mathbf{p}_r, \mathbf{p}_s, \omega) \alpha'(\mathbf{x}_s, \mathbf{p}_s, \omega) \beta'(\mathbf{x}_r, \mathbf{p}_r, \omega). \tag{C-2}$$



Substituting Equation C-2 into C-1 yields:

$$\begin{aligned}
J(m(\mathbf{x})) &= \frac{1}{2} \sum_{\omega} \sum_{\mathbf{x}_s} \sum_{\mathbf{x}_r} |c|^8 \left| \sum_{\mathbf{p}_s} \sum_{\mathbf{p}_r} r(\mathbf{p}_r, \mathbf{p}_s, \omega) \alpha'(\mathbf{x}_s, \mathbf{p}_s, \omega) \beta'(\mathbf{x}_r, \mathbf{p}_r, \omega) \right|^2 \\
&= \frac{1}{2} \sum_{\omega} \sum_{\mathbf{x}_s} \sum_{\mathbf{x}_r} |c|^8 \left( \sum_{\mathbf{p}_s} \sum_{\mathbf{p}_r} r(\mathbf{p}_r, \mathbf{p}_s, \omega) \alpha'(\mathbf{x}_s, \mathbf{p}_s, \omega) \beta'(\mathbf{x}_r, \mathbf{p}_r, \omega) \right)' \times \\
&\quad \left( \sum_{\mathbf{p}'_s} \sum_{\mathbf{p}'_r} r(\mathbf{p}'_r, \mathbf{p}'_s, \omega) \alpha'(\mathbf{x}_s, \mathbf{p}'_s, \omega) \beta'(\mathbf{x}_r, \mathbf{p}'_r, \omega) \right) \\
&= \frac{1}{2} \sum_{\omega} |c|^8 \sum_{\mathbf{p}_s} \sum_{\mathbf{p}'_s} \sum_{\mathbf{p}_r} \sum_{\mathbf{p}'_r} r'(\mathbf{p}_r, \mathbf{p}_s, \omega) r(\mathbf{p}'_r, \mathbf{p}'_s, \omega) \times \\
&\quad \sum_{\mathbf{x}_s} \sum_{\mathbf{x}_r} \alpha(\mathbf{x}_s, \mathbf{p}_s, \omega) \beta(\mathbf{x}_r, \mathbf{p}_r, \omega) \alpha'(\mathbf{x}_s, \mathbf{p}'_s, \omega) \beta'(\mathbf{x}_r, \mathbf{p}'_r, \omega), \tag{C-3}
\end{aligned}$$

where  $r(\mathbf{p}_r, \mathbf{p}_s, \omega)$  is defined to be the residual in the encoded source and receiver domain:

$$r(\mathbf{p}_r, \mathbf{p}_s, \omega) = d(\mathbf{p}_r, \mathbf{p}_s, \omega) - d_{\text{obs}}(\mathbf{p}_r, \mathbf{p}_s, \omega). \tag{C-4}$$

For plane-wave phase encoding, with sampling dense enough in  $\mathbf{x}_s$  and  $\mathbf{x}_r$ , the inner-most summations become Dirac delta functions:

$$\begin{aligned}
&\sum_{\mathbf{x}_s} \sum_{\mathbf{x}_r} \alpha(\mathbf{x}_s, \mathbf{p}_s, \omega) \beta(\mathbf{x}_r, \mathbf{p}_r, \omega) \alpha'(\mathbf{x}_s, \mathbf{p}'_s, \omega) \beta'(\mathbf{x}_r, \mathbf{p}'_r, \omega) \\
&\approx \frac{1}{|\omega|^4} \delta(\mathbf{p}'_r - \mathbf{p}_r) \delta(\mathbf{p}'_s - \mathbf{p}_s). \tag{C-5}
\end{aligned}$$

For random phase encoding, we can also approximately have

$$\begin{aligned}
&\sum_{\mathbf{x}_s} \sum_{\mathbf{x}_r} \alpha(\mathbf{x}_s, \mathbf{p}_s, \omega) \beta(\mathbf{x}_r, \mathbf{p}_r, \omega) \alpha'(\mathbf{x}_s, \mathbf{p}'_s, \omega) \beta'(\mathbf{x}_r, \mathbf{p}'_r, \omega) \\
&\approx \delta(\mathbf{p}'_r - \mathbf{p}_r) \delta(\mathbf{p}'_s - \mathbf{p}_s). \tag{C-6}
\end{aligned}$$

Therefore the data-misfit function in the encoded source and receiver domain is

$$J(m(\mathbf{x})) \approx \frac{1}{2} \sum_{\omega} |c|^4 \sum_{\mathbf{p}_s} \sum_{\mathbf{p}_r} |d(\mathbf{p}_r, \mathbf{p}_s, \omega) - d_{\text{obs}}(\mathbf{p}_r, \mathbf{p}_s, \omega)|^2. \tag{C-7}$$